Measurement of Specific Heat Functions by Differential Scanning Calorimetry

M. J. O'NEILL
The Perkin-Elmer Corp., Norwalk, Conn.

▶ When a sample material is subjected to a linear temperature program, the heat flow rate into the sample is proportional to its instantaneous specific heat. By recording this heat flow rate as a function of temperature, and comparing it with the heat flow rate into a standard material under the same conditions, the specific heat of the sample is determined as a function of temperature. The method is illustrated by measurements on various samples in the temperature range 340° to 510° K., and agreement with literature specific heat values is demonstrated. The ultimate precision of the method is 0.3% or better, which approaches the precision of adiabatic calorimetry. However, measurements may be made with samples which are four orders of magnitude smaller, and program rates two orders of magnitude larger, than those typical of conventional calorimetry.

Determination of specific heat is accomplished in two ways, depending on the temperature range in which the property is to be measured. From cryogenic temperatures to approximately 350° K., adiabatic calorimeters are used, while at higher temperatures the drop calorimeter, using the method of mixtures, is preferred. Representative adiabatic calorimeters and drop calorimeters have been described in detail in the literature (*1*, *4*, *12*).

A common feature of these calorimeters is that in order to achieve precision their applicability in routine laboratory analysis has been seriously compromised. Analysis time is prohibitively long, large samples are required, and sample geometries must be carefully controlled.

A more fundamental objection to these techniques concerns their precision at transition temperatures in the sample material. In the adiabatic calorimeter, adequate resolution of sharp transitions is possible only at extremely slow scanning rates, and with a resultant loss in sensitivity and signal-to-noise (S/N) ratio. In the drop calorimeter, heat contents referred to a standard temperature (usually 298.15° K.) are measured; transition heat effects may be obtained by comparison of heat content values on both sides of the transition temperature, but this method is unreliable when the difference is small.

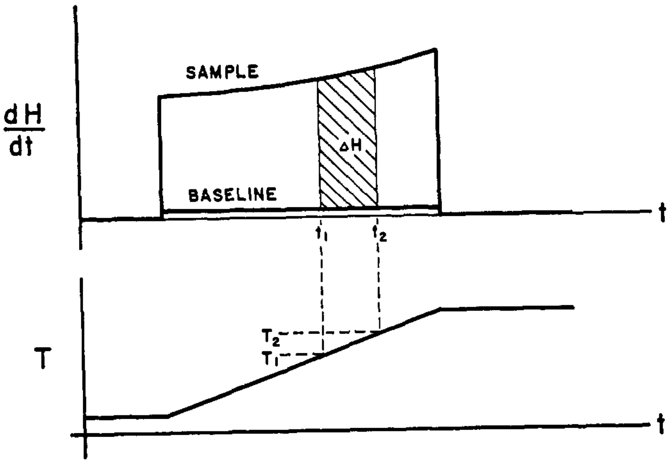

Figure 1. Linear temperature program

At temperatures above 350° K., specific heats in the absence of sharp transitions are obtained by differentiation of the algebraic function of T which best fits the measured heat content data. It is evident that this process can lead to percentage errors in the specific heat which are considerably greater than the errors in the original measurements. The advantages of a technique which would permit the direct measurement of specific heat and determination of heat content changes by integration of the specific heat function are clear.

DIFFERENTIAL SCANNING CALORIMETRY

A new instrumental method for the direct measurement of specific heat has been developed. In differential scanning calorimetry (DSC), the sample material is subjected to a linear temperature program, and the heat flow rate into the sample is continuously measured; this heat flow rate is proportional to the instantaneous specific heat of the sample (*7*, *11*).

Two sample holders are mounted symmetrically inside an enclosure which is normally held at room temperature. A primary temperature control system controls the average temperature of the two sample holders, using platinum resistance thermometers and heating elements embedded in the sample holders. A secondary temperature control system measures the temperature difference between the two sample holders, and adjusts this difference to zero by controlling a differential component of the total heating power. This differential power is measured and recorded.

SPECIFIC HEAT DETERMINATION

In order to measure the specific heat of a sample, the sample holder temperature is programmed as shown in Figure 1. To establish a base line, the program is carried out with no sample present; however, empty aluminum foil sample containers are placed in the sample holders. Isothermally, the base line indicates the differential losses of the two sample holders at the initial temperature. When the program begins, there may be a small offset from the isothermal base line, caused by the thermal capacity mismatch between the two sample holders and their contents. When the temperature program ends, the isothermal base line reappears.

This procedure is then repeated, with a weighed sample added to the sample holder. The isothermal base lines are unaffected, since the sample has no influence on the power dissipation of the sample holder. However, there is an additional offset from the programming

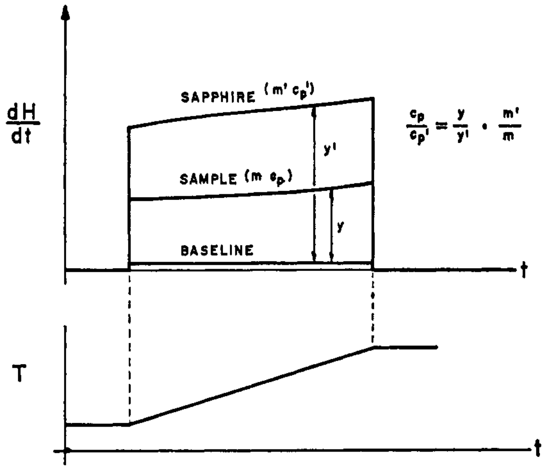

Figure 2. C_p calculation by ratio method

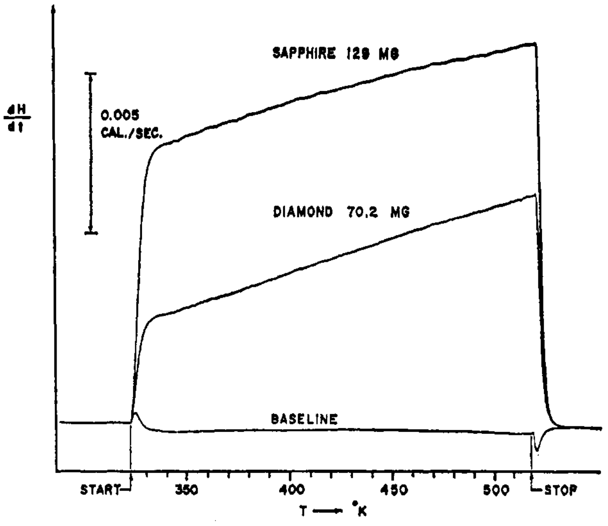

Figure 3. Base line, calibration, and sample analysis

base line, owing to the absorption of heat by the sample. If the sample is entirely enclosed by the sample holder, every elementary volume within the sample must eventually arrive at the program rate dT/dt prescribed by the sample holder, after a transient effect, the duration of which depends on the size and thermal diffusivity of the sample. Therefore the heat flow rate into the sample is given by

$$\frac{dH}{dt} = mC_p \frac{dT}{dt} \qquad (1)$$

where dH/dt is the heat flow rate in calories second^{-1}, m is the sample mass in grams, C_p is the specific heat in calories gram^{-1} ° K.$^{-1}$, and dT/dt is the program rate in ° K. sec.$^{-1}$

It follows that the area under the dH/dt curve between any two temperatures is the change in heat content, as shown by Equation 2:

$$H(T_2) - H(T_1) = \int_{t_1}^{t_2} \frac{dH}{dt}\, dt \qquad (2)$$

This illustrates the difference between scanning calorimetry and the drop calorimeter technique, where the heat content is the measured property, and the specific heat is obtained by differentiation.

Although every part of the sample is programming at exactly the same rate dT/dt, the true temperature of the sample differs slightly from the indicated temperature of the sample holder, owing to temperature gradients which appear within the sample and at the interface between the sample and the sample holder. The gradient at the interface is always much larger than the gradient within the sample, and is one of the sources of error to be discussed later.

In order to use Equation 1 in a specific heat calculation, the ordinate calibration and the temperature program rate must be known with at least the precision required of the final result. However, these two parameters may be eliminated from the calculation if a material with a known specific heat is used to calibrate the instrument. Such a material is α-aluminum oxide, or synthetic sapphire, for which the specific heat has been determined to five significant figures in the temperature range 0° to 1200° K. (*3*).

Figure 2 illustrates the method. After the base line and sample programs, a third program is run with a weighed sapphire standard. At any temperature T, the following equations apply:

$$Ky = mC_p \frac{dT}{dt} \qquad (3)$$

$$Ky' = m'C_p' \frac{dT}{dt} \qquad (4)$$

where y and y' are the ordinate deflections in inches due to the sample and the standard, respectively, m' and C_p' are the mass and specific heat of the standard, and K is the ordinate calibration factor, in cal. inch^{-1} sec.$^{-1}$

Dividing Equation 3 by Equation 4, and rearranging terms:

$$\frac{C_p}{C_p'} = \frac{m'y}{my'} \qquad (5)$$

Thus the calculation requires only the comparison of two ordinate deflections at the same temperature. It will be observed that the calculation would be correct even if the ordinate calibration and the program rate were temperature-dependent. In fact, the ordinate calibration varies by less than 2% over the operating temperature range of the instrument. However, the program rate may vary by as much as 5% in a 100° K. interval, owing to the inevitable nonlinearities in the temperature calibration and in the temperature control system. Thus Equation 5 represents the better method of calcula-

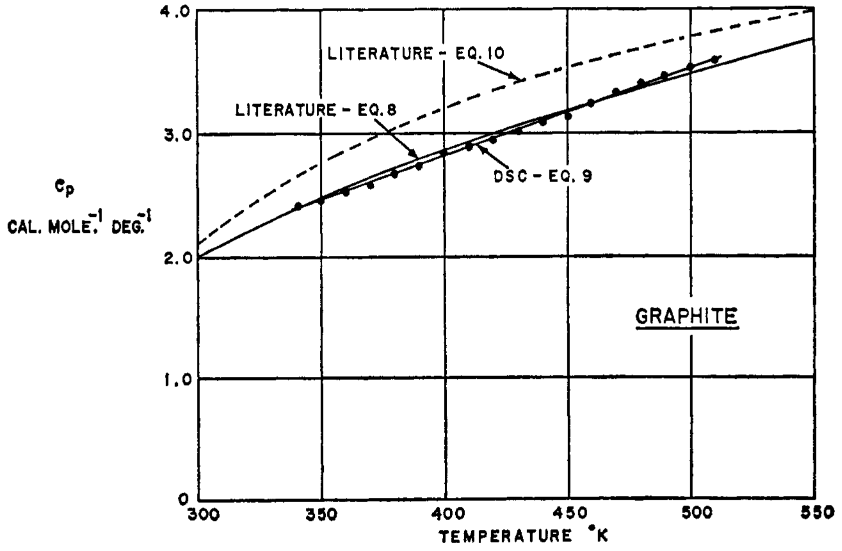

Figure 4. Specific heat of graphite, 39.7 mg.

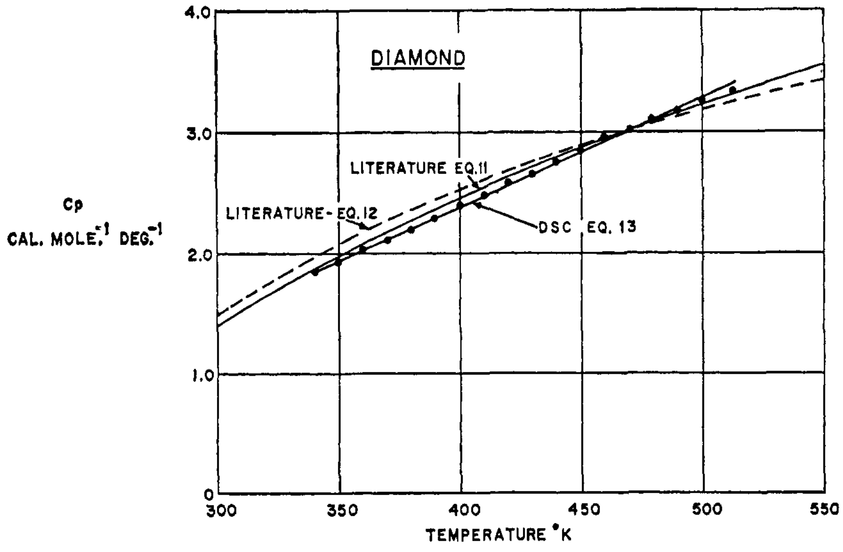

Figure 5. Specific heat of diamond, 70.2 mg.

tion. For repetitive determinations at a single temperature, Equation 1 might be used with a calibration factor, but with a considerable loss of accuracy.

EXPERIMENTAL

The procedure described above was carried out with the Perkin-Elmer Model DSC-1, on a number of samples for which specific heat functions have been measured by other investigators. A temperature interval from 340° to 510° K. was used for all but one of the measurements to be discussed, where a slightly smaller interval was used. The nominal program rate was 20° K. minute^{-1}.

At the beginning and end of each program there are characteristic transient behaviors of the base line, associated with the distributed thermal capacity of the sample holders. In order to give the initial transient behavior time to disappear, the temperature program was started at 320° K. The analysis time was approximately 15 minutes, including 2 minutes of isothermal recording at the initial and final temperatures. Between analyses, 15 minutes were allowed for the surrounding enclosure to return to its original temperature distribution.

All samples were encapsulated in the aluminum foil dishes supplied with the instrument, which weigh approximately 20 mg. with their covers. It was verified by calculation that the small weight variations between these dishes would contribute a negligible error to the measurement.

It is important to cover the sample holders with the metallic covers provided. This ensures that the isothermal base line is unaffected by the presence or absence of sample. A front panel control is provided to adjust for the unbalance between the sample holder losses at any temperature; this control was used to make the base lines at 320° and 510° K. coincide.

The sapphire heat capacity standard was supplied with the instrument, and had a weight of 129 mg. The temperature scale was calibrated with melting point standards.

The ordinate data were recorded with a Leeds and Northrup Speedomax G 10-mv. recorder, with a chart speed of 1 inch per minute. A full scale deflection corresponded to a differential heat flow rate of 1.4×10^{-2} cal. sec.$^{-1}$, except for one sample ($AgNO_3$), where twice this sensitivity was used.

RESULTS AND DISCUSSION

Figure 3 illustrates a typical base line, sapphire calibration, and sample analysis. The base line shows a downscale capacity offset of approximately 4×10^{-4} cal. sec.$^{-1}$, which was left uncorrected. The ordinate calibration is shown for reference.

For each sample, C_p was calculated at intervals of 10°, using the method of Equation 5, and the data were plotted against a temperature abscissa. Figures 4 and 5 show the calculated specific heat functions for graphite and diamond. These samples are unusual, in that their specific heats are quite small and very temperature-dependent.

In accordance with the suggestion of Maier and Kelley (*6*), the heat content and specific heat functions of such samples are usually represented by expressions of the form

$$H(T) - H(T_0) = aT + \frac{b}{2}T^2 + cT^{-1} - d \quad (6)$$

$$C_p = a + bT - cT^{-2} \quad (7)$$

The four coefficients are chosen so that the function described by Equation 6 matches the measured heat content function as closely as possible. Table I shows the comparison between the DSC data and literature values for these samples. The first literature function for each sample was calculated from recent heat content measurements between 298° and 600° K. (*2, 9, 10*), while the second is the equation given by Kelley (*5*), covering a much wider temperature interval.

Equations 9 and 13 are linear approximations to the DSC data, obtained by the least squares method. For graphite, the greatest departure from

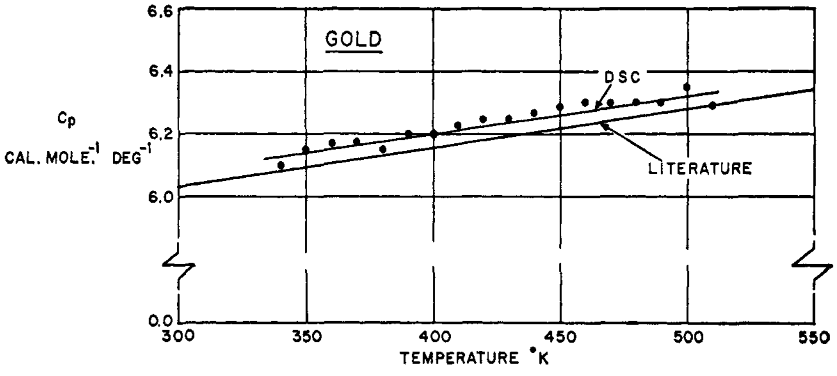

Figure 6. Specific heat of gold, 657 mg.

Table I. Specific Heat Functions

(Cal. mole^{-1} ° K.$^{-1}$)

	Graphite	Diamond
Literature^a	$1.56 + 4.53 \times 10^{-3}T - 8.22 \times 10^{4}T^{-2}$ (Eq. 8)^c	$1.10 + 5.14 \times 10^{-3}T - 1.11 \times 10^{5}T^{-2}$ (Eq. 11)^d
Literature^b	$4.03 + 1.14 \times 10^{-3}T - 2.04 \times 10^{5}T^{-2}$ (Eq. 10)^c	$2.27 + 3.06 \times 10^{-3}T - 1.54 \times 10^{5}T^{-2}$ (Eq. 12)^d
DSC	$-0.03 + 7.12 \times 10^{-3}T$ (Eq. 9)^c	$-1.15 + 8.85 \times 10^{-3}T$ (Eq. 13)^d

[a] 298–600° K.
[b] 298–2500° K. for graphite, 298–1200° K. for diamond.
[c] See Figure 4.
[d] See Figure 5.

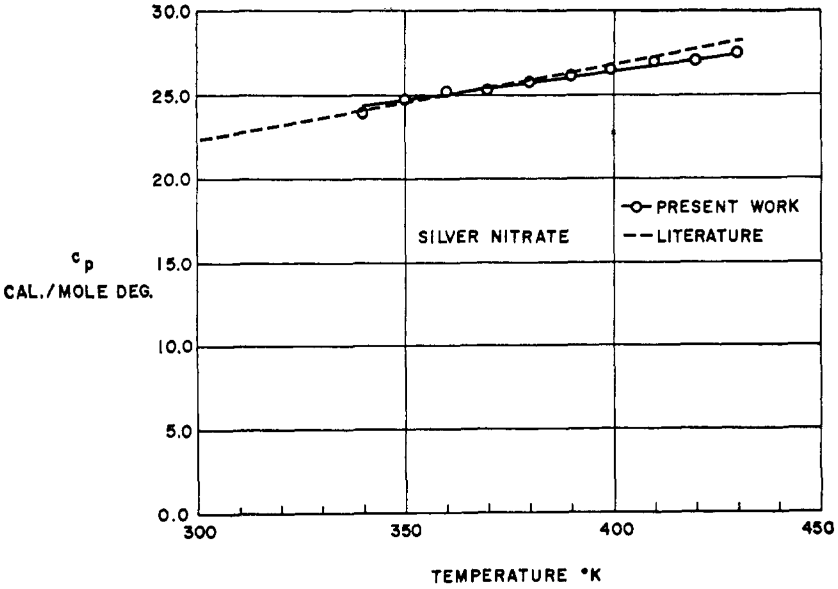

Figure 7. Specific heat of silver nitrate, 55.9 mg.

the literature (Equation 8) is 1.4%, at 390° K. For diamond, the greatest departure is 3.0%, at the same temperature. These literature values are shown as solid curves in Figures 4 and 5.

The broken curves in Figures 4 and 5 represent the wide temperature interval approximations (Equations 10 and 12). With only four coefficients available in the empirical heat-content equation, the curve-fitting error must increase without limit as the temperature interval is increased.

Table II shows specific heat functions for pure gold, fully annealed, and for silver nitrate. Figure 6 shows the data for gold and the literature data, with an expanded ordinate scale to show the temperature dependence of specific heat more clearly. The agreement with the literature is within 0.7%. Figure 7 shows the data for silver nitrate; for this sample the error approaches 2.5% at 430° K.

The behavior of silver nitrate is shown in Figure 8. Although the sample was programmed to a temperature well above its melting point of 484° K., specific heat calculations were made only for the α-phase, from the initial temperature to 433° K., owing to the anomalous behavior of the α–β transition at this temperature. This transition, unlike the fusion, was not reversible when the sample temperature was programmed back to 320° K., and there were some indications of rate-dependent behavior.

At the transition and fusion temperatures for this sample, the apparent thermal capacity dH/dT is far greater than mC_p, and the calorimeter was driven into saturation. This accounts for the poor resolution of these transitions in the 55.9-mg. sample. In order to observe such transitions, smaller samples should be used, as demonstrated by the second silver nitrate analysis superimposed on the first one. This recording was made with a sample weighing 0.55 mg. As anticipated, the ordinate deflection due to mC_p is almost indistinguishable from the base line, whereas the fusion is well resolved, with a S/N ratio greater than 100. Better temperature resolution would be obtained at slower programming rates, at the expense of S/N ratio.

The α-β transition was not resolved any better with the smaller sample size, and disappeared entirely when the analysis was repeated. Further study of this behavior was considered to be outside the scope of the investigation.

The last sample to be studied was a polycarbonate resin, which displays a characteristic jump in specific heat at the glass transition temperature. It is in the analysis of phenomena such as this one that the direct measurement of specific heat is most valuable. With the drop calorimeter method, the location and magnitude of the transition would have to be inferred from a small change in the slope of the heat content function, and a number of heat content measurements would have to be made at temperatures close to the glass transition.

The analysis can be made with a scanning adiabatic calorimeter, provided that very slow scanning rates, typically 20° K. per hour or less, are used. Figure 9 shows the analysis of a polycarbonate sample on the DSC-1, with a sample weight of 42.8 mg. Figure 10 shows the specific heat function calculated for this sample, and for

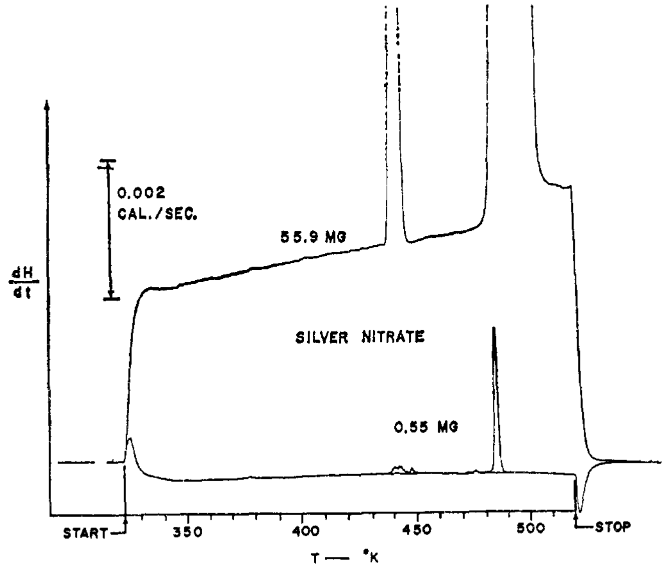

Figure 8. Silver nitrate analysis, showing influence of sample size

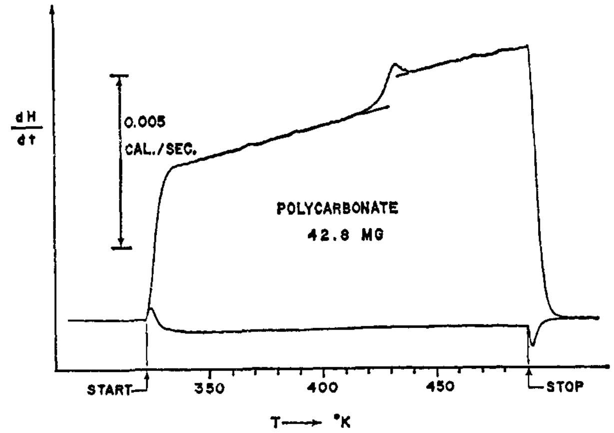

Figure 9. Polycarbonate analysis

comparison the data from a recent determination with an adiabatic calorimeter (*8*). The agreement is within 2% below the glass transition temperature, and within 4% at higher temperatures. The close agreement may be fortuitous, since there probably were differences in structure or crystallinity between the two samples.

The present work indicates that the specific heat of this material increases from 0.41 to 0.47 cal. gram^{-1} ° K.$^{-1}$ in a transition temperature interval between 420° and 430° K. The ordinate accuracy could be improved with faster program rates or a larger sample, at the expense of temperature resolution. The exchange of temperature resolution for S/N ratio is inherent in scanning calorimetric methods.

One advantage of differential calorimetry appears in the analysis of small phenomena superimposed on a changing total specific heat. For example, the slowly varying component of the specific heat of the polycarbonate may be suppressed in the readout by placing in the reference holder a suitable quantity of a material which has a similarly varying specific heat without any transitions. The step function in the polycarbonate specific heat will then appear on a flat base line, and thus may be examined with greater ordinate sensitivity.

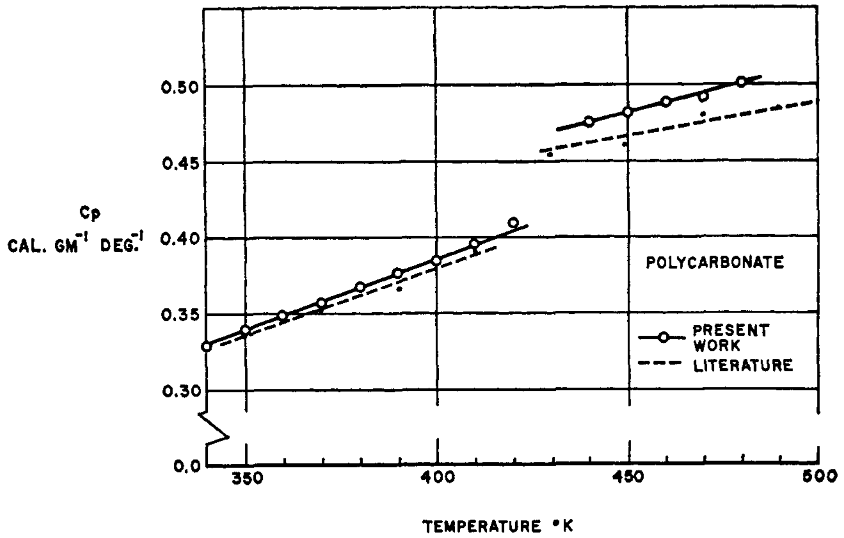

Figure 10. Specific heat of polycarbonate

SOURCES OF ERROR

The specific heat measurement described above is based on the comparison of the heat flow rates into sample and standard materials subjected to identical temperature programs. The limiting sources of error are the random noise on the measured ordinate deflection and the reproducibility of the temperature program, which is essentially the random noise on the abscissa.

There are also systematic errors, such as those caused by ordinate nonlinearity and inaccurate temperature calibration, which can be reduced to any desired level at the expense of analysis time. The ordinate linearity of the calorimetric readout is within 1%, and will not introduce an appreciable error if the sample size is chosen so that the ordinate deflections for sample and reference materials are similar. The temperature scale is calibrated with melting point standards, and the errors of interpolation can be minimized by calibrating at smaller intervals. These methods are time-consuming, and are justified only for measurements of the highest accuracy.

Returning to the nonsystematic errors, we consider first the ordinate noise level. This is specified by the manufacturer as less than 8×10^{-5} cal. sec.$^{-1}$ peak-to-peak. For a S/N ratio of 100, the sample size and scanning rate should therefore be chosen for a heat flow of 1.6×10^{-2} cal. sec.$^{-1}$ In this case, the ordinate deflections may be established with an uncertainty of ±0.5%, and their ratio therefore has an uncertainty of ±1.0%.

Actually, this is a conservative estimate of the possible error, since specific heat functions vary slowly with temperature, and a smooth curve may be drawn which is a much better approximation to the true ordinate deflection than implied above. For the most precise work, the analysis may be repeated one or more times, and the data from successive runs may be averaged.

The second nonsystematic error is due to the imperfect reproducibility of the temperature program. The reproducibility of the sample holder temperature is of the order of 0.1° K., which generates negligible errors in specific heat measurements. However, the true sample temperature differs from the sample holder temperature during a program, owing to the temperature gradient across the finite resistance between the sample and the sample holder. This resistance is approximately 100° K. sec. cal.$^{-1}$, and is reproducible within about 25%. Thus there might conceivably be a difference of 50° K. sec. cal.$^{-1}$ between sample and standard coupling resistances, which at a heat flow rate of 1.6×10^{-2} cal. sec.$^{-1}$ would cause a total abscissa error of 0.8° K. The resulting specific heat error depends upon the slope of the specific heat functions of the sample and standard materials. If the true temperature of the sapphire standard differs by 0.4° K. from the indicated temperature, the ordinate error will be 0.04%, since the specific heat of sapphire has a slope of approximately 0.1%° K.$^{-1}$ in the temperature range covered by the DSC-1. The additional error due to the sample temperature error of 0.4° K. in the other direction may be estimated similarly.

The magnitude of the abscissa error is directly proportional to the heat flow rate into the sample, while the error due to the ordinate noise level is inversely proportional to the same heat flow rate. The overall error is minimized when the operating conditions are adjusted so that the errors contributed by these two sources are equal. With careful handling of samples and data reduction, an uncertainty of ±0.3% in specific heat may be realized. On the other hand, determinations of specific heat with an uncertainty no greater than 3% may be made in little more than the time required to weigh the sample and scan its temperature through an interval of 20 ° K.

Table II. Specific Heat Functions

(Cal. mole^{-1} °K.$^{-1}$)

	Gold	Silver nitrate
Literature	$5.66 + 1.24 \times 10^{-3}T$	$8.76 + 4.52 \times 10^{-2}T$
DSC	$5.71 + 1.23 \times 10^{-3}T$	$12.27 + 3.55 \times 10^{-2}T$

The experimental work described above lies between these two extremes; the temperature scale was calibrated with three standards over a range of 180° K, and the abscissa accuracy is estimated to be within 1° K. There was no attempt to match sample and standard heat flow rates, and there was no averaging of data from successive analyses on any sample. Under these conditions, the accuracy of the specific heat functions determined above is estimated to be within ±1.0%.

LITERATURE CITED

(1) Dauphinee, T. M., MacDonald, D. K. C., Preston-Thomas, O., *Proc. Roy. Soc. (London)* **221**, 267 (1954).
(2) Evans, W. H., NBS *Rept.* **6928** (1960).
(3) Furukawa, G. T., Douglas, T. B., McCoskey, R. E., Ginnings, D. C., *J. Res. Natl. Bur. Std.* **57**, 67 (1956).
(4) Ginnings, D. C., Corruccini, R. J., *Ibid.*, **38**, 593 (1947).
(5) Kelley, K. K., *U. S. Bur. Mines Bull.* **584** (1960).
(6) Maier, C. G., Kelley, K. K., *J. Am. Chem. Soc.* **54**, 3243 (1932).
(7) O'Neill, M. J., ANAL. CHEM. **36**, 1238 (1964).
(8) O'Reilly, J. M., Karasz, F. E., Bair, H. E., *J. Polymer Sci., Part C*, Polymer Symp., No. 6 (1963).
(9) Stull, D. R., JANAF Thermochemical Data (1961).
(10) Victor, A. C., *J. Chem. Phys.* **36**, 1903 (1962).
(11) Watson, E. S., O'Neill, M. J., Justin, J., Brenner, N., ANAL. CHEM. **36**, 1233 (1964).
(12) Westrum, E. F., Jr., Hatcher, J. B., Osborne, D. W., *J. Chem. Phys.* **21**, 419 (1953).

RECEIVED for review March 29, 1966. Accepted June 22, 1966.

Differential Thermal Analysis–Effluent Gas Analysis Method for Identification and Determination of Nitrides in Steel

W. R. BANDI, W. A. STRAUB, E. G. BUYOK, and L. M. MELNICK
United States Steel Corp., Applied Research Laboratory, Monroeville, Pa.

▶ A DTA–EGA technique has been developed for the determination of specific nitrides in residues extracted from steel. The method can be used to identify nitride phases in steel which are not identifiable by any other analytical procedure. The procedure can be used to detect as little as 5 μg. of nitrogen. Other compounds present in the extracted residue did not interfere with the nitrogen determination. Above 10 μg. an accuracy within 10% of the amount present appears to be possible.

METALLURGICAL literature shows that more than 30 nitrogen-bearing compounds have been identified or postulated to exist in steels that are produced today. From consideration of the composition of these steels and reference to the thermodynamics for the formation of nitrides, it appears possible that as many as 75 simple and complex nitrogen compounds may exist in various steel alloys now manufactured. These compounds are known to affect the physical and mechanical properties of steel.

Although the effects of nitrides are at least partially known for simple steel-alloy systems, they have not been extensively studied in complex ferrous alloys mainly because of the lack of a good analytical method for determining which nitrides are present. At least 25 nitride-forming elements are used in various types of steels and eight or 10 may be used in a single type. The problem is further complicated by the fact that metal carbides, sulfides, or oxides of the same elements may also be present. Thermodynamics can be used to predict which compounds might occur, but without knowledge of kinetics these predictions are unreliable, and compounds are found in steel that would appear to be thermodynamically impossible.

Optical and electron microscopy, x-ray and electron diffraction, the electron microprobe, chemical analysis, and combinations of these techniques have been used to gain analytical information about compounds in steel. All of these are useful, but they have limitations in terms of applicability. For instance, the resolution of optical microscopy is limited, and poor diffraction patterns are obtained when the particles are fine. (Particles of carbides and nitrides as small as 100 A. have been found in steel.) Furthermore, diffraction patterns of phases may not be identified if the constituent is present as less than about 5% of a residue extracted from the steel. Also, some carbides and nitrides have similar diffraction patterns.

Beeghly's ester-halogen extraction method (*4*) and methods for the determination of acid-soluble (*6*, *7*) and/or heat-treatable nitrogen (*9–12*) have been used in many past metallurgical investigations of nitrides, but as the alloy system increases in complexity, the information gained by these methods is less specific. Therefore, for the past several years we have been investigating the possibility of using differential thermal analysis–effluent gas analysis (DTA–EGA) to analyze for compounds that can be extracted from steel. Our preliminary work with extracted residues has been reported previously (*1–3*, *13*). Also, preliminary experiments with an EGA analytical train were reported by Garn (*8*) in 1964. This work discloses the design and testing of a DTA–EGA system that will detect 10 μg. or more of nitrogen in milligram quantities of residue extracted from steel.

EXPERIMENTAL

DTA Apparatus. R. L. Stone Model 12BC$_2$. The DTA assembly was modified for these experiments as follows:

Copper tubing ($^1/_8$-inch o.d.) was soldered to the pressure regulator of the oxygen tank and a needle valve capable of controlling the dynamic oxygen flow at 3 ml. per minute was substituted for the gas controls in the furnace platform.

A modified sample holder assembly (Figure 1) was fabricated from Inconel. Salient features of the design include a small effluent gas volume to attain the desired EGA sensitivity, gas seals away from the heated area to ensure a minimum gas leakage, and a stacked thermocouple arrangement to hold platinum dishes containing the sample and reference material. The stacked thermocouple is part of a bridge circuit containing the thermocouple beads.

To facilitate use of the sample holder assembly, a hole was drilled through the top of the DTA furnace. An asbestos washer was placed on top of the furnace and around the sample holder assembly. To protect the gas seals from heat a split water jacket made of copper was clamped around the tubing between the asbestos washer and the gas seal.

EGA Train. The assembly for the determination of nitrogen in the effluent gas is shown in Figure 2. To maintain a small gas volume, minimum lengths of $^1/_8$-inch o.d. copper